Article:

Gan, Y., Chen, X., Tong, Y. et al. (2 more authors) (2018) Thermal performance of a meso-scale combustor with electrospray technique using liquid ethanol as fuel. Applied Thermal Engineering, 128. pp. 274-281. ISSN 1359-4311

https://doi.org/10.1016/j.applthermaleng.2017.09.016

Thermal performance of a meso-scale combustor with electrospray technique using liquid ethanol as fuel

Y.H. Gan[1,*], X.W. Chen[1], Y. Tong[1], X. Zhang[1], Y. Zhang[2,]**

1. School of Electric Power, South China University of Technology, Guangzhou 510640, China

2. Department of Mechanical Engineering, The University of Sheffield, Sheffield, S1 3JD, UK;

Submitted for publication in

Applied Thermal Engineering

*Corresponding author: Prof. Y.H. Gan, Ph.D.,

Address: School of Electric Power, South China University of Technology, Wushan Road, Tianhe District, Guangzhou 510640, China

Tel/Fax: 00-86-20-87110613

Email: ganyh@scut.edu.cn.

**Corresponding author: Prof. Y. Zhang, Ph.D.,

Address: Department of Mechanical Engineering, The University of Sheffield, Sheffield, S1 3JD, UK

Tel/Fax: 00-44-1142227880

Email:yz100@sheffield.ac.uk

Highlights:

1. Thermal performance of a meso-scale combustor is evaluated experimentally.

2. The flame was anchored near the steel mesh in combustor.

3. Thermal efficiencies are from 21.96% to 41.83% under different equivalence ratios.

4. Heat recirculation zone is found near to the mesh and improve the combustion.

Abstract

A new meso-scale combustor to be coupled with energy conversion modules was fabricated. The volume of the combustor was on the order of a few cubic centimeters. Ethanol was applied as fuel and electrosprayed at the flow rate of 3.5ml/h. Stable flame which shaped in a rounded slice was achieved near the mesh as equivalence ratios varying from 0.9~1.7 without external heating and catalyst. The temperatures of flame, combustor outer wall and exhausted gas were measured. Flame temperatures were within the range of 1100 K to 1300 K. Exhausted gas components were detected by a gas chromatograph and the combustion efficiencies were estimated in the range of 51.18% to 92.43%. Heat losses from the combustor wall were calculated and accounted for about 35% of input energy. The combustion efficiency and flame temperature reached their maximum values of 92.43 % and 1287.26 K respectively at equivalence ratio = 1.0. The outer wall temperature distributions along the flow direction were measured and heat recirculation zone was found about 10mm in the upstream of the mesh, which was beneficial for stable combustion. The steel mesh not only helped to gather charged droplets as a collector but also act as a flame holder. Thermal efficiency exceeded 21.0% and maximal thermal efficiency was up to 48.8%.

Keywords: meso-scale combustion; electro-spraying; heat loss; combustion efficiency; thermal efficiency

1. Introduction

Micro/meso-combustion has attracted more and more attention with the development of manufacturing and miniaturization of equipment. Chemical batteries are still the most used power source for electronic products. Though great progress have been made in battery technology, such as fast recharging, new materials of electrodes, the energy density of batteries is extremely limited compared to liquid fuels [1]. Power sources with high specific energy and small volume are in great need. Micro combustion is a feasible way to fulfill energy conversion in a compact area with high energy density and durability.

A comprehensive review of fundamentals, devices and applications on micro combustion can be seen in [1, 2]. Combustion in micro scale faces many difficulties due to scaling effects. Surface-to-volume ratio is increased dramatically which results in high heat loss ratio [3]. Short residence times on micro and meso scale combustors lead to incomplete conversion of fuels [4]. To establish stable combustion in a micro combustor, numerous experimental researches were carried out, and gas fuels were applied for most condition. Heat recirculation and external heating are common and effective methods to reduce heat losses. Heat recirculation which means that enthalpy from burned gas was recirculated to preheat reactants, was widely used in research jobs [5, 6]. External heating of combustor can prevent flame from quenching in an internal diameter smaller than quenching diameter [7, 8, 9]. The combustor geometry is essential to the mixture of fuel and oxides and extension of residence time. A backward-facing step applied in the combustor can significantly improve performance in many aspects [10, 11, 12].The performance of mixed fuels combustion was also investigated [13, 14, 15]. Different from gas fuels, fine evaporation is a prerequisite of liquid fuel combustion. Porous media and film combustion was used to enlarge surface area and prolong residence time [16-19]. Gan et.al developed a micro combustor using electrospray technique for liquid fuel combustion [20]. Liquid fuel was dispersed into droplets thus evaporation rate increased greatly, and the electrospray was studied [21, 22]. Based on the previous work about micro combustion and combustors, some energy conversion modules were developed. Contributions in this field can be divided into two categories. The first category is known as direct energy conversion module, for example, a thermoelectric (TEG) or thermophotovoltaic (TPV) generator. Direct energy conversion system is easy to be fabricated and operated. A crucial disadvantage of direct energy conversion system is its particularly low efficiencies which were less than 15% [23 - 25]. Another category involves the modules based on conventional power cycles, such as gas turbines, internal combustion engines and Stirling engines [26 - 28]. In this method, challenges lies in balancing rotary parts and fabrication technologies as well as sealing difficulties. Comparatively high efficiencies make them a feasible way to be a miniaturized power source for practical use with high energy density.

Micro and meso combustor is a key component of miniaturized power system. The combustor in present study is considered to be coupled with anenergy conversion module based on conventional cycle. The emphasis falls on the combustion design to burn liquid fuel with electrospray technique in a volume on the order of a few cubic centimeters. Quenching problems should be considered at sub-millimeter dimension [29], thus quenching problems can be ignored in this study. In order to combust liquid fuel in meso-scale, the combustor using electrospray technique was fabricated. To characterize the performance of the combustor, flame temperatures were measured, the heat losses by radiation and convection were calculated, and combustion efficiency and thermal efficiency were investigated.

2. Experimental setup

The schematic diagram of the meso-scale combustion system is shown in Fig.1. The whole system is exposed to the ambient. It consists of a two high voltage power sources, an air tank, a mass flow controller, a syringe pump, a meso-combustor, a PC, an IR camera, a gas chromatograph (GC) and several connection tubes. Ethanol is chosen to be the fuel because of its high heat value, low boiling point, fast evaporation rate and it is renewable and environmental friendly. The flow rate of ethanol is controlled by a syringe pump (KDS100, KDScientific) with accuracy to ±1% of the full scale. The flow rate of air (20% O_2, 80% N_2) is accurately adjusted by a mass flow controller (Brooks5850E, Brooks) with an uncertainty of ±1%. The two-dimensional temperature distribution of the outer wall was recorded by an IR camera (PM575, FLIR) with an uncertainty of ±0.1 K. It is noted that the measured surface temperature is strongly depended on the surface emissivity. Other factors, such as the ambient temperature, the air humidity and distance between the camera lens and the tube surface can be accurately measured. The infrared signal will have reflection and refraction on the surface of quartz tube, thus the measurement of IR camera will resulted in unacceptable errors. To avoid the problem and enhance the accuracy of measurement, the quartz tubes were painted with black lacquer. The temperature measurements were calibrated by an S-type thermocouple coated on the outer wall surface. The emissivity of the black lacquer is about 0.90~0.93 with temperatures in the range of 1100 K ~ 1300 K. The variation in terms of temperature readings caused by two different emissivity values is about 3~ 5 K, depending on the temperature magnitude (the higher the temperature, the larger the variation). Thus the overall uncertainty of IR camera is within ±0.5%. Flame temperatures and exhausted gas temperatures were measured by an S-type thermocouple. Five points on the flame front surface as shown in Fig.2 were selected for temperature measurement. The average temperature of the five points was considered as flame temperature. The bead diameter of the thermocouple is 0.3mm, which is much small compared to the diameter of flame, so the influence of thermocouple on the flame can be negligible. In present study, all flame and gas temperatures were fixed by taking the radiation heat loss of thermal couple into account. And the uncertainty of flame and gas temperature measurements after correction was less than ±0.7%. The main components of the exhaust gas were detected by a gas chromatograph (GC1690, Kexiao, China). All measurements were done after a steady-state combustion was achieved, which is estimated by the temperature readings (≤ 2K fluctuation) at different points of combustor wall.

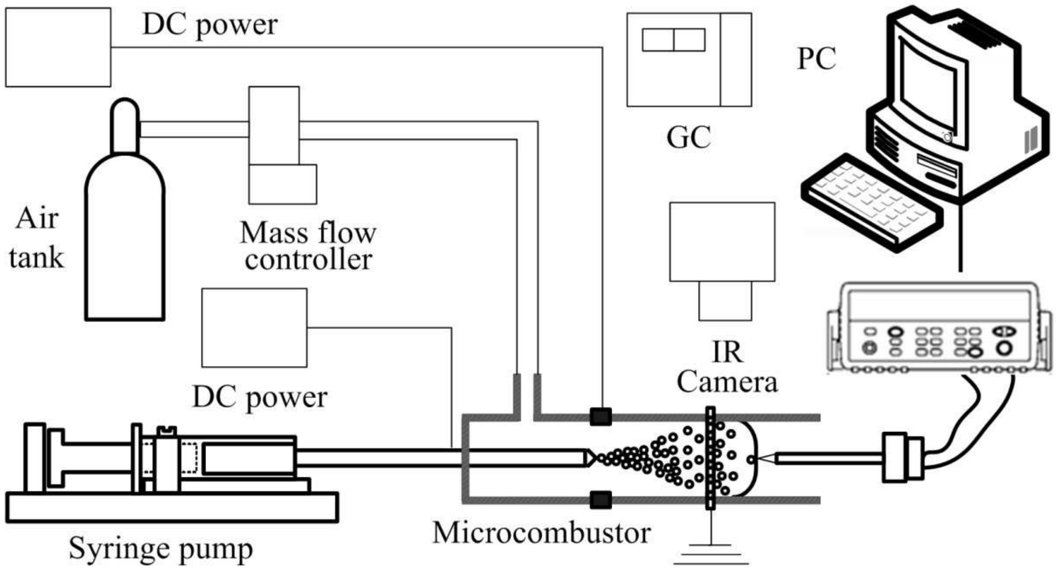

Fig.1. Schematic diagram of the meso-scale combustion system

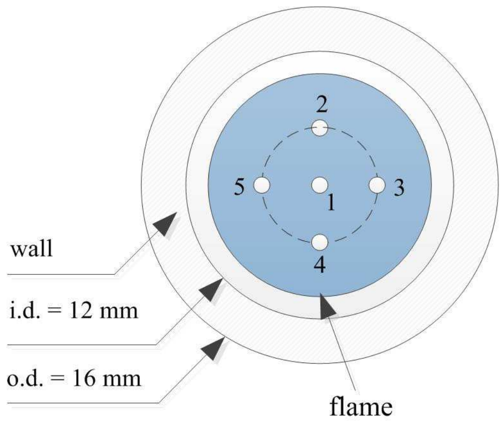

Fig.2. Schematic diagram of measuring points (1 ~ 5) on flame front surface

The schematic diagram of the meso-scale combustor is shown in Fig.3. It consisted of a steel capillary nozzle, a ring electrode, a steel mesh and quartz tubes. The tip of the steel nozzle was 1.1 mm away from the left side of the ring electrode. The inner diameter of air inlet is 5 mm. The inner and outer diameters of the capillary nozzle are 0.9mm and 1.1mm respectively. The capillary nozzle is connected to a DC power source with the voltage of V_c. And the ring electrode was connected to another DC power source with the voltage of V_r. The steel mesh is grounded and used as ethanol droplets collector. If the steel mesh is not grounded or taken away, the electrospray will flow back to the ring electrode and result in wall-wetting. Liquid fuel combustion with high efficiency requires sufficient evaporation rate. Electrospray technique can produce quasi-monodispersed and homopolarly charged droplets at a small flow rate. Ethanol droplets are easy to evaporate at ambient temperature, and homopolar charges prevent droplets from coalescence. The velocity of droplets is about 2.5m/s measured by PDA (Dantec, Denmark), which enhances the mixture of air and fuel. Liquid ethanol was atomized between the tip of capillary nozzle and grounded mesh under the combined electric field. An alcohol burner was used to ignite the ethanol at the end of combustor after the mixture of air and fuel spray. The combustor was set up horizontally for the convenience of ignition, and once the stable flame was formed, the combustion process was self-sustained and the alcohol burner was no needed any more.

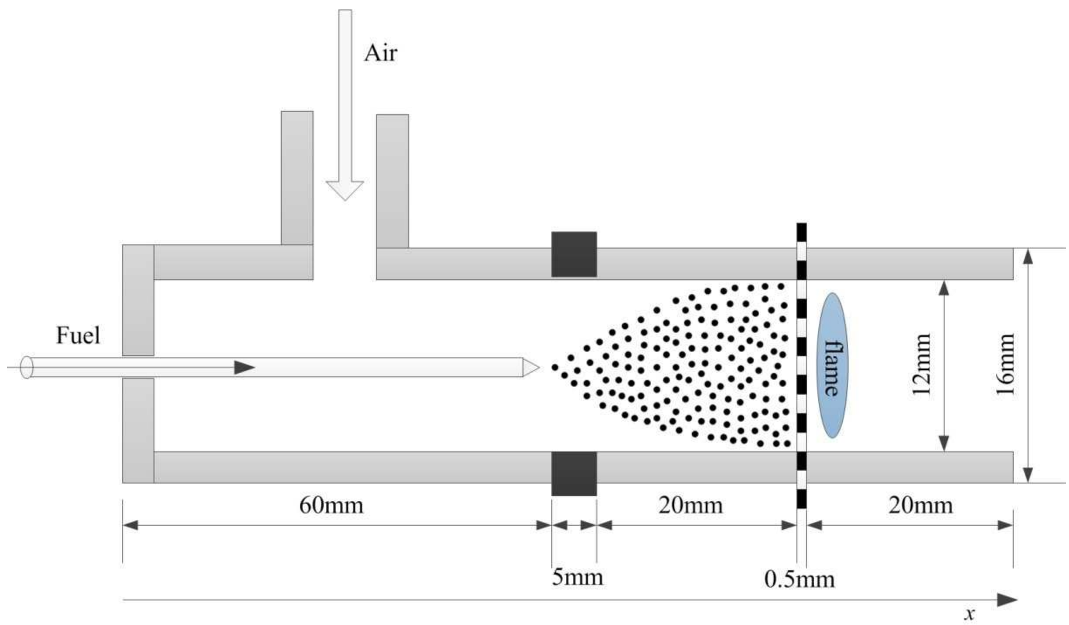

Fig.3. Schematic diagram of the meso-scale combustor

3 Results and Discussion

The investigation of ethanol electrospray can be found in literature [21, 22]. The atomization pattern of the ethanol spray was shown in Fig.4, which was taken without quartz tube and in the absence of combustion. Similar images were also taken with quartz tubes (without black lacquer painted) during combustion process, while the images were less informative because the reflections on the quartz tubes. Similar electrospray structure was also formed by observing. The operating conditions in present study were as follows: fuel flow rate q_v=3.5 ml/h, voltage on nozzle V_c=5.50 kV, voltage on ring electrode V_r= 1.25 kV, and the equivalence ratio ϕ = 0.90~1.70. The fuel flow rate and voltages were kept unchanged during experiment. In terms of fuel flow rate, some efforts were made to choose an appropriate one. The flame cannot be ignited at fuel flow rate less than 2.0ml/h. Wall wetting phenomenon occurred at fuel flow rate larger than 6.0ml/h for the present single capillary spray system.

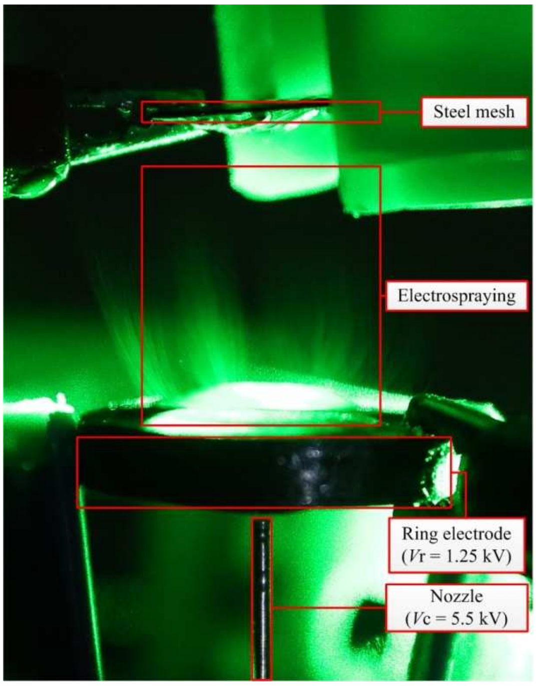

Fig.4. Electrospray structure of ethanol into ambient air condition

(q_v=3.5ml/h, V_c=5.50kV, V_r=1.25kV)

3.1Combustion process and temperature distributions

Fig.5 showed the flame images (front view) and infrared images (side view) of wall temperature distributions under different equivalence ratios. The side view of the flame cannot be taken because the quartz tubes were painted with black lacquer. During the experimental process, it was found that the flame could not be ignited when the dry air flow rate was too low. When the flow rate of dry air was increased to a certain value, a stable flame could be ignited by an alcohol burner. Once a stable flame was established, the heat source was not needed any more and the combustion would continue until all fuel was consumed. The flame is shaped in a "rounded slice" near the mesh. The diameter of the flame increased with the increasing air flow rate which can be easily observed from Fig.5. The color of the flame changed from light blue to blue which implied the improvement of combustion efficiency. The flame was blown off as ϕ approaching below 0.9. The high velocity of the reactants prevented the flame from anchoring near the mesh.

The flame temperatures varied from 1100 K to 1300 K under different equivalence ratios as shown in Fig.6, which were able to couple an energy conversion module using conventional cycles and it was safe for the materials. Appropriate flame temperature can prevent combustor from burnout.

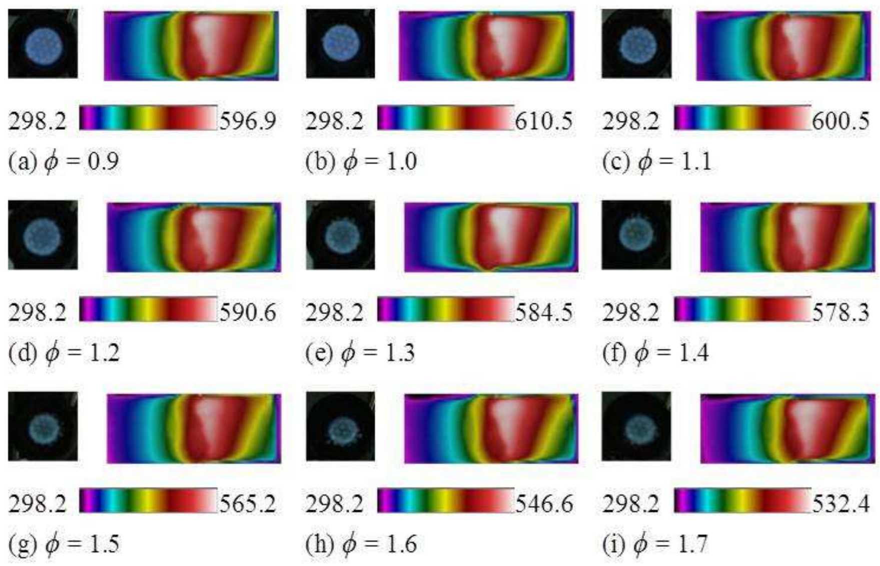

Fig.5. Flame images and infrared images under different equivalence ratios (In Kelvin temperature, q_v=3.5 ml/h, V_c=5.50 kV, V_r=1.25kV)

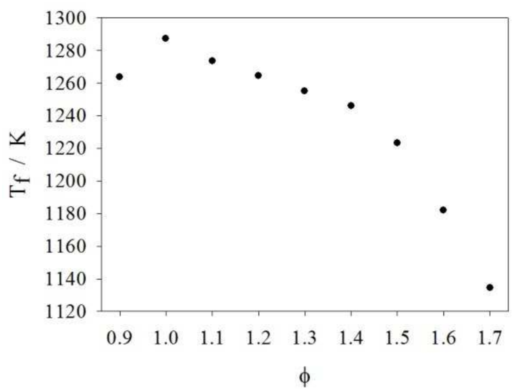

Fig.6. Flame temperatures under different equivalence ratios (q_v=3.5 ml/h, V_c=5.50 kV, V_r=1.25 kV)

Each pixel of infrared image represented the temperature of the specific area of the wall. Since the wall temperature is close to ambient temperature at the left side of ring electrode, heat losses from the left side of ring electrode were omitted. And the error caused by the ignorance is less than 5%. The actually considered area was

16mm×40mm and 30×75 pixels on the IR images. Heat losses from the wall consisted of natural convection heat loss and radiation heat loss. The wall can be discretized into 30×75elements. The radiation heat loss Q_{rad} was given by the radiation law of Stefan-Boltzmann:

$$Q_{\mathrm{rad}} = 2\sum \varepsilon\sigma A_i[(T_i)^4 - (T_0)^4] \quad (1)$$

Where ε is the emissivity of the wall, σ is Stephen-Boltzmann constant equals to 5.67×10^{-8}W/m^{2}K^4, A_i is area of element$i$, T_i is the temperature of element$i$.

The actual area is larger than 16mm×40mm because the combustor wall is cylindrical in shape, and it has to be considered in the calculation of A_i. As depicted Fig.7, the line AD in IR image was actually the arch $\widehat{\mathrm{AB}}$ of the combustor, and the line DE was actually the arch $\widehat{\mathrm{BC}}$. The outer diameter of the combustor was divided into 30sections with equal length in the IR image. While its actual length was the length of the arch, here is an example of calculating the length of the arch $\widehat{\mathrm{BC}}$. And the length of each arch can be calculated using the same method.

$$\widehat{\mathrm{BC}} = \widehat{\mathrm{AC}} - \widehat{\mathrm{AB}} = r(arccos\angle\mathrm{AOC} - arccos\angle\mathrm{AOB}) \quad (2)$$

$$\widehat{\mathrm{BC}} = r\left(arccos\frac{r-\mathrm{AE}}{r} - arccos\frac{r-\mathrm{AD}}{r}\right) \quad (3)$$

In the equations above r is the outer radius of the combustor. The length of AD and AE can be easily solved because the outer diameter was divided into 30sections with equal length.

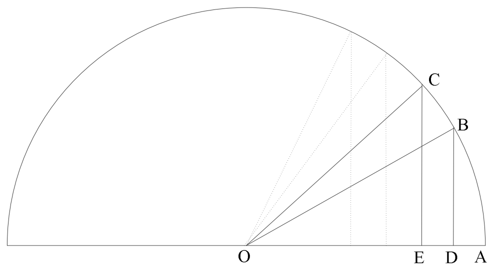

Fig.7. The schematic of calculating the length of arch $\widehat{\mathrm{BC}}$

The precise determination of natural heat convection heat loss was a rather difficult job. While using the classic experimental correlation formula with considerable accuracy is a feasible way to estimate the heat loss by natural convection.

Natural convection heat loss (Q_{nc}) can be calculated as:

$$Q_{\mathrm{nc}} = 2hA(T_{\mathrm{m}} - T_0) \tag{4}$$

Where$h$ is natural heat transfer coefficient, A is half area of combustor wall, $T_m$is the mean temperature of the wall, T_0 is the ambient temperature.

Natural heat transfer coefficient was calculated by the following correlation formula [30],

$$h = \lambda \cdot 0.48(G_r \cdot P_r)^{0.25}/d \tag{5}$$

$$G_r = gl^3\alpha_v\Delta t/v^2, P_r = v/a \tag{6}$$

where, Gr is the Grashof number corresponding to the wall temperature, Pr is the Prandtl number of air,g is gravity acceleration,d is the outer diameter of combustor,$\alpha_\upsilon$is volume expansion coefficient, Δt is the difference of wall temperature and ambient temperature, υ represents kinematic viscosity, a is thermal diffusivity of air and$\lambda$is the thermal conductivity of air. The magnitude of h is about 12.5 W/m^{2}K, according to literature, the heat transfer coefficient was usually selected between 10 ~ 20 W/m^2K [18, 31]. Thus the calculation of h in the present study was convincing..

The wall heat losses Q_{loss} were the sum of radiation heat loss Q_{rad} and natural convection Q_{nc}:

$$Q_{\text{loss}} = Q_{\text{rad}} + Q_{\text{nc}} \quad (7)$$

Heat losses under different equivalence ratios were shown in Fig.8. In this study, the power of convection and radiation were very close. For some combustors with high temperatures, the radiation heat transfer was much larger than the convection heat transfer [32-34] because the convection heat loss is proportional to T, while the radiation heat loss is proportional to T^4. The wall temperature of the present combustor was relatively low when compared to TPV systems, usually up to1500K [5, 24, 25]. The magnitude of heat losses calculated based on the IR images ranged from 6.66 W to 9.94 W. A simple calculation can be done to quantify the ratio of heat losses. The heat value of ethanol is 29700kJ/kg. The possible maximal power of the combustor was 22.8 W if the ethanol was combusted with efficiency of 100%. The ratio of heat losses was in the range of 29.2%~43.6%, and it would be larger if the combustion efficiency was considered.

It can be seen from Fig.5 that the shape of the flame was nearly a circle under all conditions with different diameters, hence thewall temperature distribution shared asimilar pattern. The wall temperature increased along x direction and reached maximum value near the flame, and then decreased. Larger flame indicated more heat generation, higher flame temperature and wall temperature and more heat losses. The heat losses reached their maximum at ϕ= 1.0 and then decreased as ϕ changed. For ϕ> 1,the fuel was unable to combust completely with insufficient air supply, which resulted in less heat generation, so the heat losses were decreased with the increasing of equivalence ratio. The heat losses were also decreased as ϕ<1, thiswas mainly caused by the decrease of residence time with high air velocity. In order to reduce the heat losses, some suggestions were proposed in literature, such as choosing wall materials with lower thermal conductivity and coating a layer of special material with lower emissivity [32].

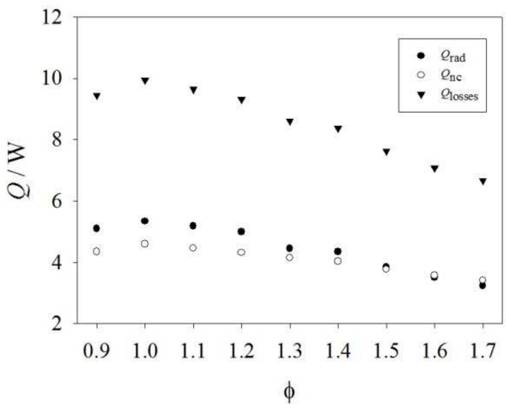

Fig.8. Heat losses under different equivalence ratios

(q_v=3.5 ml/h,V_c=5.50 kV,V_r=1.25kV)

The axial temperatures of wall were depicted in Fig.9. Each temperature distribution curve showed a similar tendency. The highest wall temperature always reached near the flame which was a few millimeters away from the mesh. For many combustors using gas fuels, the flame location would shift with the air velocity [35], while in the present study, the flame location was always located near the mesh in all experimental conditions, and just shifted slightly with different air flow rate, this was important for a combustor to couple with an energy conversion module. The mesh played a crucial role in stabilizing the flame. The mesh was designed to collect chargeddroplets, but it can also act as a flame holder.

The combustor can be generally divided into three regimes, preheating zone (from the tip of capillary to the mesh), burning zone (from the mesh to the position of highest temperature where $\frac{dT_{\mathrm{w}}}{dx} = 0$) and exhaust zone (from the end of burning zone to the end of the combustor). The burning zone was where heat was generated, the energy was transferred to the preheating zone and exhausted zone. The exhausted gas was in high temperature, thus the exhausted gas may transfer its energy to the wall. Heat recirculation from wall to the mixture of fuel and air was supposed to be existed in the preheating zone. To determine whether heat recirculation existed, control volume of the combustor wall was selected to analyze the heat exchanges in different zones. Control volume was shown in Fig.10, the energy balance equation can be described as:

$$Q_{\mathrm{R}} + Q_{\mathrm{mw}} = Q_{\mathrm{L}} + Q_{\mathrm{c}} + Q_{\mathrm{r}} \tag{8}$$

Where Q_{mw} represents the heat exchange between the mixture (air and fuel) and combustor wall, Q_{R} and Q_{L} represents the heat exchange at the right and left boundary respectively, Q_{c} and Q_{r} represents the heat transfer of convection and radiation from the combustor wall. The positive direction is supposed to be consistent with the arrows in Fig.10.

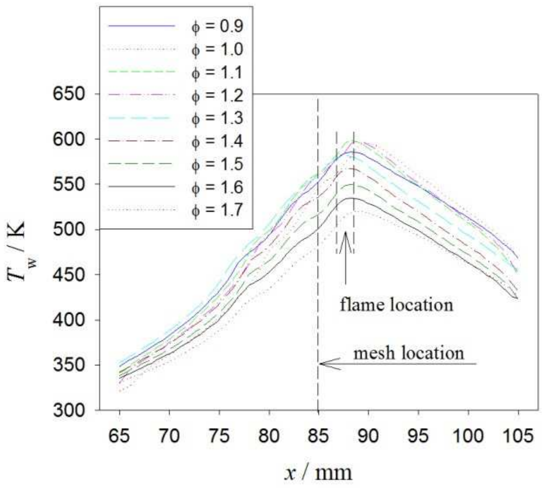

Fig.9. Wall temperature distribution along x direction under different equivalence ratios (q_v=3.5 ml/h,V_c=5.50 kV,V_r=1.25kV)

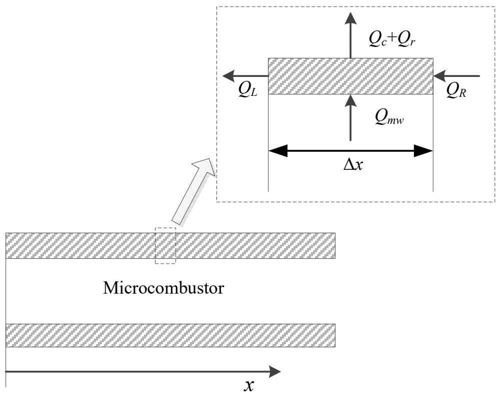

Fig.10. Schematic of control volume of combustor wall

From Eq. (8), it could be derived,

$$Q_{\mathrm{mw}} = Q_{\mathrm{c}} + Q_{\mathrm{r}} - (Q_{\mathrm{R}} - Q_{\mathrm{L}}) \tag{9}$$

The wall temperature is always higher than the ambient temperature, which implies,

$$Q_{\mathrm{c}} + Q_{\mathrm{r}} > 0 \tag{10}$$

$$Q_{\mathrm{c}} + Q_{\mathrm{r}} = (h_{\mathrm{c}} + h_{\mathrm{r}})(T_{\mathrm{w}} - T_{\mathrm{o}})\Delta x \tag{11}$$

$$h_{\mathrm{r}} = \sigma\varepsilon(T_{\mathrm{w}} + T_{\mathrm{o}})(T_{\mathrm{w}}^2 + T_0^2) \tag{12}$$

Then Eq. (11) can be rewritten as:

$$Q_{\mathrm{c}} + Q_{\mathrm{r}} = [h_{\mathrm{c}} + \sigma\varepsilon(T_{\mathrm{w}} + T_{\mathrm{o}})(T_{\mathrm{w}}^2 + T_0^2)](T_{\mathrm{w}} - T_{\mathrm{o}})\Delta x \tag{13}$$

According to Fourier's law of heat conduction,

$$Q_{\mathrm{R}} - Q_{\mathrm{L}} = \left[\left(\frac{\mathrm{d}T_{\mathrm{w}}}{\mathrm{d}x}\right)_{\mathrm{R}} - \left(\frac{\mathrm{d}T_{\mathrm{w}}}{\mathrm{d}x}\right)_{\mathrm{L}}\right] \times \lambda_{\mathrm{w}} \times \delta = \frac{\mathrm{d}^2 T_{\mathrm{w}}}{\mathrm{d}x^2} \times \Delta x \times \lambda_{\mathrm{w}} \times \delta \tag{14}$$

Where λ_{w} is the thermal conductivity of the combustor wall, δ (=2mm) is the thickness of the combustor wall, $\frac{d^2 T_{\mathrm{w}}}{dx^2}$ is the gradient of $\frac{dT_{\mathrm{w}}}{dx}$.

Then the expression of Q_{mw} can be written as:

$$Q_{\mathrm{mw}} = [h_{\mathrm{c}} + \sigma\varepsilon(T_{\mathrm{w}} + T_{\mathrm{o}})(T_{\mathrm{w}}^2 + T_0^2)](T_{\mathrm{w}} - T_{\mathrm{o}})\Delta x - \frac{\mathrm{d}^2 T_{\mathrm{w}}}{\mathrm{d}x^2} \times \lambda_{\mathrm{w}} \times \delta \times \Delta x \tag{15}$$

With the analysis above, Q_{mw} can be calculated quantitatively. The heat exchange characteristics were analyzed at different zone based on the wall temperature gradient.Select the experimental data and combustion condition of ϕ= 0.9 as an example of data processing.The wall temperature gradient atϕ=0.9and 1.5was drawn in Fig.11. Not all temperature gradientcurves under different equivalenceratios were plotted for readability, some of the curves overlapped with each other. But all the temperature gradient curves shared the similartendency due to the similarwall temperature distribution (shown in Fig.9) under all experimental conditions.

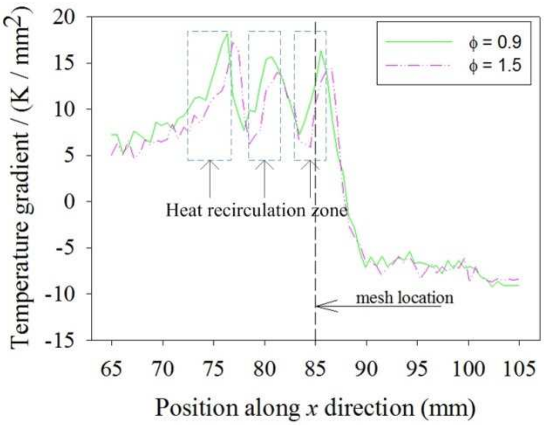

Fig.11. The temperature gradient at ϕ= 0.9 and 1.0

(q_v=3.5 ml/h,V_c=5.50 kV, V_r=1.25kV)

At 65mm <x< 70mmand x> 90mm, the temperature gradient almost kept constant, implying

$$Q_R - Q_L \approx 0 \tag{16}$$

$$Q_{mw} = Q_c + Q_r - (Q_R - Q_L) \approx Q_c + Q_r > 0 \tag{17}$$

The direction of heat exchange was from mixture of fuel and air to combustor wall at the region 65mm <x< 70mm and x> 90mm. At x near 75 mm, 80mm and 85mm, the temperature gradient increasedalong the positive direction of x, which indicates,

$$\left(\frac{\mathrm{d}T_w}{\mathrm{dx}}\right)_R > \left(\frac{\mathrm{d}T_w}{\mathrm{dx}}\right)_L, Q_R - Q_L > 0 \tag{18}$$

The direction of Q_{mw}cannot be determined directly, according to Eq. (9), select a control volume at78mm <x<80mm as an example,

h_c=12.5W/m^{2}K, ε=0.9, T_w =561.10 K, $\frac{d^2T_w}{dx^2}$=4.23 K/mm^2, λ_w=1.46W/mK.

Q_{mw} = 7937.34Δx - 12351.64Δx < 0

The direction of Q_{mw} is negative, which indicates that the heat transfer direction was from the combustor wall to the mixture of fuel and air. Heat recirculation occurred at $x$near 75 mm, 80mm and 85mm. Though the calculation may not be exactly precise, it provided a feasible way to determine where the heat recirculation between wall and mixtures occurred.

The same calculations were done to the rest experimental conditions. It was found that Q_{mw} was always negative at x near 75 mm, 80mm and 85mm, which indicated that the heat recirculation occurred at those regions. Heat recirculation was beneficial for the preheating of reactants, especially for the evaporation of liquid fuel. It can be seen that at x between 85 mm ~ 90 mm, the temperature gradient was decreasing, which means the heat transfer direction is from the mixture of fuel and air to the combustor wall. Because the flame with high temperature was anchored at x between 85 mm ~ 90 mm, the mixture of fuel and air with high temperature transferred its energy to the wall.Heat recirculation was about 10mm in length in the upstream of the mesh based on the analysis above.

3.2 Combustion efficiency and Thermal efficiency

Combustion efficiency and thermal efficiencywere the two key parameters to be considered. Gas chromatographic measurements of the main components such as CO, CO_2 and N_2 in the dry sample of exhausted gas were conducted. Some products may not be detected by GC such as CH_4 and unburned ethanol.Theseproducts were calculated into the unburned ethanol based on the balance of carbon.

Combustion efficiency was defined as:

$$\eta_c = \frac{m_f Q_e - m_e Q_e - m_{co} Q_{co}}{m_f Q_e} \tag{19}$$

Where m_f is the mass of fuel, m_e and m_{co} are the mass of ethanol and CO in the exhausted gas. Q_e and Q_{co} is the lower heat value of ethanol and CO.

The combustor was designed to be coupled with an energy conversion module based on conventional cycles, the gained enthalpy contained in the exhausted gases can be utilized, and thus the thermal efficiency was defined as:

$$\eta_t = \frac{\sum c_{pi} m_i (T - T_0)}{m_f Q_e} \tag{20}$$

$\sum c_{pi} m_i (T - T_0)$ means the gained enthalpy of exhausted gas, i is different gas species such as N_2, O_2, CO_2, H_2O, C_2H_5OH and CO. c_{pi} is the specific heat at constant pressure. m_i is the mass of species i. T is the temperature of exhausted gas.

Performing the standard error analysis gave the accuracies of the combustion efficiencies of ±1.21%, and the thermal efficiencies of ±1.13%.

Fig.12 showed the calculated combustion efficiencies and thermal efficienciesof the combustor under different equivalence ratios based on the experimental results. The measured CO concentrations were less than 1% under all conditions, which indicated the combustor was environmental friendly. The color of the flame was blue, so there was no soot formation. Highest combustion efficiency was reached at ϕ = 1.0. The combustion efficiency decreased as the equivalence ratio increased.Insufficient air flow rate resulted in the drop of combustion efficiency, the ethanol cannot combusted completely and some of the gas evaporated by liquid ethanol was brought to the ambient. There was also a drop at ϕ = 0.9, this was mainly caused by the decrease of residence time with a comparatively higher air velocity. The experiments were carried out at a given fuel flow rate, the equivalence ratio was controlled by adjusting the air flow rate the velocity of the fuel and air mixture$\upsilon \propto q$, the residence time $\tau \propto \frac{1}{\upsilon}$, thus$\tau \propto \frac{1}{q}$. The residence time decreased with the increasing air flow rate. The less the residence time, the less the mixing and reaction time. Substantial mixing of fuel and air and adequate residence time are the prerequisites of complete combustion. The decreased residence time resulted in the decrease of flame temperature and combustion efficiency. Many researchers studied the combustion efficiency of gas fuels, but few investigated the liquid fuel combustion efficiency in micro and meso scale combustion. The highest combustion efficiencies of gas fuels may exceed 99% in different combustors [32, 33,36]. For liquid fuels, there are some inevitable problems such as fuel dispersion and evaporation, which resulted in lower efficiencies compared to gas fuels. Thermal efficiencies showed a similar trend as combustion efficiencies.As it was shown in Fig.12, maximal thermal efficiency was 48.83% at ϕ = 1.0 and minimum thermal efficiency was 21.97% at ϕ = 1.7. J. Li et al [37] studied a planar combustor for a TPV system, and the highest emitter efficiency of the micro-combustor was 22.5%.The combustor was promising to be coupled with energy conversion modules with a considerable efficiency.

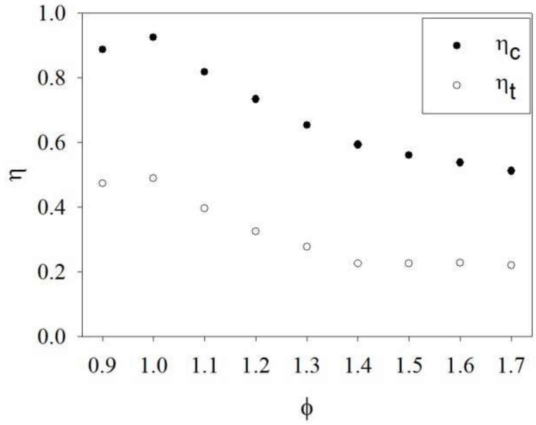

Fig.12. Combustion efficiencies and thermal efficiencies under different equivalence ratios (q_v=3.5 ml/h,V_c=5.50 kV,V_r=1.25kV)

4 Conclusions

Anew meso-scale combustor was designed and made in this study. Liquid fuel is favored by its high heat value. Electrospray technique was applied to disperse liquid fuel to accelerate its evaporation process. Stable flame was established under equivalence ratios ranging from 0.9 to 1.7. The mesh not only helped to gather charged droplets as a collector but also acted as a flame holder. Heat recirculation occurred under all experimental conditions, which was beneficial to the evaporation of liquid fuel. The thermal efficiency of the combustor exceeded 21.97% and up to 48.83%. The flame temperature, heat losses, combustion efficiencies and thermal efficiencies all reached maximal value at $\phi = 1$. These characteristics of stable flame location, appropriateflame temperature and high efficiencies made the combustor using electrospray method a good choice for energy conversion module at micro and meso scales.

Acknowledgements

The authors gratefully acknowledge the National Nature Science Foundation of China (51376066, 51611130194), and State Key Laboratory of Engines, Tianjin University (K2016-01).

Reference

[1] Y.G. Ju, K. Maruta. Microscale combustion: Technology development and fundamental research, Prog. Energy. Combust. Sci 37 (2011) 669-715

[2] N.S. Kaisare, D.G. Vlachos. A review on microcombustion: Fundamentals, devices and applications, Prog. Energy. Combust. Sci 38 (2012) 321-359

[3] J.L. Wan, A.W. Fan, Y. Liu, H. Yao, W. Liu, X.L. Gou, D.Q. Zhan, Experimental investigation and numerical analysis on flame stabilization of CH4/air mixture in a mesoscale channel with wall cavities, Combust. Flame 162 (2015) 1035-1045

[4] C.M. Miesse, R.I. Masel, C.D. Jensen, M.A. Shannon, M. Short, Submillimeter-scale combustion, AIChE Journal 50 (2004) 3206-3214

[5] F.J. Weinberg, D.M. Rowe, G. Min, P.D. Ronny. On thermoelectric power conversion from heat recirculating combustion systems, Proc. Combust. Ins 29 (2002) 941-947

[6] S.K. Som, U. Rana. Wall heat recirculation and exergy preservation in flow through a small tube with thin heat source, Int. Commun. Heat Mass. 64 (2015) 1-6

[7] K. Maruta, T. Kataoka, N.I. Kim, Minaev S, Fursenko R. Characteristics of combustion in a narrow channel with a temperature gradient, Proc. Combust. Inst 30

(2005) 2429-2436.
[8] A.W. Fan, S. Minaev, S. Kumar, W. Liu, K. Maruta. Regime diagrams and characteristics of flame patterns in radial microchannels with temperature gradients, Combust. Flame 153 (2008) 479–489
[9] D.S. Annalisa, C. Christian, D. Guillaume, D. Philippe. Combustion in micro-channels with a controlled temperature gradient, Exp. Therm. Flu. Sci 73 (2016) 79-86
[10] W.M. Yang, S.K. Chou, C. Shu, Z.W. Li, H. Xue. Combustion in micro-cylindrical combustors with and without a backward facing step, App. Therm. Eng 22 (2002) 1777-1787
[11] B. Khandelwal, A. A.Deshpande, S Kumar. Experimental studies on flame stabilization in a three step rearward facing configuration based micro channel combustor, App. Therm. Eng 58 (2013) 363-368
[12] M Baigmohammadi, S Tabejamaat, Y Farsuani. Experimental study of the effects of geometrical parameters, Reynolds number, and equivalence ratio on methane–oxygen premixed flame dynamics in non-adiabatic cylindrical meso-scale reactors with the backward facing step, Chem. Eng. Sci 132 (2015) 215-233
[13] A.K. Tang, J.F. Pan, W.M. Yang, Y.M. Xu, Z.Y. Hou. Numerical study of premixed hydrogen/air combustion in a micro planar combustor with parallel separating plates, International Journal of Hydrogen Energy 40 (2015) 2396 - 2403
[14] X. Li, J. Zhang, H.L. Yang, L.Q. Jiang, X.H. Wang, D.Q. Zhao. Combustion characteristics of non-premixed methane micro-jet flame in coflow air and thermal

interaction between flame and micro tube, App. Therm. Eng 112 (2017) 296 - 303

[15]A.K. Tang, Y.M. Xu, C.X. Shan, J.F. Pan, Y.X. Liu.A comparative study on combustion characteristics of methane, propane and hydrogen fuels in a micro-combustor,International Journal of Hydrogen Energy 40 (2015) 16587 - 16596

[16] X.F. Huang, S.J. Li. Ignition and combustion characteristics of jet fuel liquid film containing graphene powders at meso-scale, Fuel 177 (2016) 113-122

[17] A Sirignano. Flame structure in small-scale liquid film combustors, Proc. Combust. Inst 31 (2007) 3269-3275

[18]Y. Liu, A.W. Fan, H. Yao, W Liu. A numerical investigation on the effect of wall thermal conductivity on flame stability and combustion efficiency in a mesoscale channel filled with fibrous porous medium, Appl. Therm. Eng 101 (2016) 239-246

[19]X. Li, L. Jia, H. Nakamura, T. Tezuka, S. Hasegawa, K. Maruta. Study on flameresponses and ignition characteristics of $CH_4/O_2/CO_2$ mixture in a micro flowreactor with a controlled temperature profile, Appl. Therm. Eng 84 (2015)360 - 367.

[20] Y.H. Gan, Y. Tong, Y.G. Ju, X. Zhang, H.G. Li, X.W. Chen. Experimental study on electro-spraying and combustion characteristics in meso-scale combustors, Energy Conversion and Management 131 (2017) 10-17

[21] Y.H. Gan, X. Zhang, H.G. Li, Y. Tong, Y. Zhang, Y.L. Shi, Yang. Effect of a ring electrode on the cone-jet characteristics of ethanol from electro-spraying combustor, Journal of Aerosol Science 98 (2016) 15-29

[22] Y.H. Gan, Z.B. Luo, Y.P. Cheng, J.L. Xu. The electro-spraying characteristics of

ethanol for application in a small-scale combustor under combined electric field, App. Therm. Eng 87 (2015) 595-604

[23] J.H. Park, J.S. So, H.J. Moon, O.C. Kwon. Measured and predicted performance of a micro-thermophotovaltaic device with a heat-recirculating micro-emitter, Int J Heat Mass Transfer 54 (2011) 1046-1054

[24] J. Li, S.K. Chou, Z.W. Li, W.M. Yang. A potential heat source for the micro-thermophotovaltaic (TPV) system, Chem. Eng. Sci 64 (2009) 3282-3289

[25] G. Colangelo, A.D. Risi, D. Laforgia. Experimental study of a burner with high temperature heat recovery system for TPV applications, Energy Conversion and Management 47 (2006) 1192-1206

[26] A.C. Fernandez-Pello. Micropower generation using combustion: issues and approaches, Proc. Combust. Ins 29 (2002) 883-899

[27] A. Mehra, X. Zhang, A.A. Ayon, I.A. Waitz, M.A. Schmidt, C.M. Spadaccini. A six-wafer combustion system for a silicon micro gas turbine, Journal of Microelectromechanical Systems 9 (2000) 517-527

[28] H.T. Aichimary, D.B. Kittelson, M.R. Zachariah. Miniature free-piston homogeneous charge compression ignition engine-compressor concept part I: performance estimation and design considerations unique to small dimensions, Chem. Eng. Sci 57 (2002) 4167-4171

[29] J. Jarosinski. A survey of recent studies on flame extinction, Prog. Energy. Combust. Sci 12 (1986) 81-116

[30] S.M. Yang. Improvement of the basic correlating equations and transition criteria

of natural convection heat transfer, Heat Transfer - Asian Research 30 (2001) 293 - 399

[31] D.G. Jiang, W.M. Yang, K.J. Chua, J.Y. Ouyang. Thermal performance of micro-combustors with baffles for thermophotovoltaic system, App. Therm. Eng 61 (2013) 670 – 677

[32] H.L. Cao, J.L. Xu. Thermal performance of a micro-combustor for micro-gas turbine system, Energy Conversion and Management 48 (2007) 1569- 1578

[33] S. Yuasa, K.Oshimi, H. Nose, Y. Tennichi. Concept and combustion characteristics of ultra-micro combustors with premixed flame, Proc. Combust. Ins 30 (2005) 2455- 2462

[34] J.W. Li, B.J.Zhong. Experimental investigation on heat loss and combustion in methane/oxygen micro-tube combustor. App. Therm. Eng 28 (2008) 701- 716

[35] U.W. Taywade, A.A. Deshpande, S. Kumar. Thermal performance of a micro combustor with heat recirculation, 109 (2013) 179 – 188

[36]J.L. Wan, A.W. Fan, H. Yao, Y. Liu. Effect of thermal conductivity of solid wall on combustion efficiency of a micro-combustor with cavities, Energy Conversion and Management 96 (2015) 605- 612.

[37] J. Li, S.K. Chou, Z.W. Li, W.M. Yang. Experimental investigation of porous media combustion in a planar micro-combustor, Fuel 89 (2010) 708 - 715

List of figure captions

Fig.1. Schematic diagram of the meso-scale combustion system

Fig.2. Schematic diagram of measuring points on flame front surface

Fig.3. Schematic diagram of the meso-scale combustor

Fig.4. Electrospray structure of ethanol into ambient air condition

Fig.5. Flame images and infrared images under different equivalence ratios (In Kelvin temperature, q_v=3.5 ml/h, V_c=5.50 kV, V_r=1.25 kV)

Fig.6. Flame temperatures under different equivalence ratios (q_v=3.5 ml/h,V_c=5.50 kV,V_r=1.25 kV)

Fig.7. The schematic of calculating the length of arch $\widehat{BC}$

Fig.8. Heat losses under different equivalence ratios (q_v=3.5 ml/h,V_c=5.50 kV,V_r=1.25 kV)

Fig.9. Wall temperature distribution along x direction under different equivalence ratios (q_v=3.5 ml/h,V_c=5.50 kV,V_r=1.25kV)

Fig.10. Schematic of control volume of combustor wall

Fig.11. The temperature gradient at ϕ= 0.9 and 1.0(q_v = 3.5 ml/h,V_c= 5.50 kV,V_r= 1.25kV)

Fig.12. Combustion efficiencies and thermal efficiencies under different equivalence ratios (q_v=3.5 ml/h,V_c=5.50 kV,V_r=1.25 kV)